EPR of Mn^{2+} in the Tutton salts $M(NH_4)_2(SO_4)_2 \cdot 6H_2O$ (M = Cd, CO, Ni): Mn^{2+}-Ni^{2+} exchange interaction

Sushil K. Misra and Stefan Z. Korczak*
Physics Department, Concordia University, 1455 de Maisonneuve Boulevard West, Montreal, Quebec H3G 1M8, Canada
(Received 30 July 1986)

X-band EPR measurements on Mn^{2+}-doped isostructural single crystals of three Tutton salts $M(NH_4)_2(SO_4)_2 \cdot 6H_2O$ (M = Cd, Co, Ni) at room, liquid-nitrogen, and liquid-helium temperatures are presented. Accurate values of the Mn^{2+} spin Hamiltonian parameters in these hosts, at various temperatures, have been estimated by the use of a recently developed, rigorous, least-squares fitting procedure, especially adapted to the electron-nuclear spin-coupled system of Mn^{2+}. The absolute signs of the parameters are estimated from the relative intensities of lines at liquid-helium temperature and the spread of various fine-structure sextets. From the g shift in the paramagnetic host (M = Ni), from that in isostructural diamagnetic hosts, the average nearest- and next-nearest-neighbor Mn^{2+}-Ni^{2+} exchange interaction has been estimated to be 0.009 GHz. Linewidth variation in the paramagnetic hosts (M = Co, Ni) as a function of temperature, as well as the magnitude of external magnetic field intensity, has also been studied.

I. INTRODUCTION

Some EPR studies on Mn^{2+}-doped single crystals of the Tutton salts $M(NH_4)_2(SO_4)_2 \cdot 6H_2O$, ($M$ = Cd, Co, Ni) have been previously reported.[1-5] In the $Ni(NH_4)_2(SO_4)_2 \cdot 6H_2O$ host (hereafter NiASH) the EPR measurements were made by Upreti[1,2] at X band, and confined to room temperature (RT) only. He estimated the spin-Hamiltonian parameters (SHP) employing perturbation expressions, using only the resonant line positions obtained for $\mathbf{H} \| \hat{\mathbf{x}}$ ($\mathbf{H}$ stands for the external magnetic field). Specifically, he found (i) a monotonic increase of linewidth with the magnitude of $\mathbf{H}$, (ii) a negative shift in the g value from those in other isostructural diamagnetic Tutton salts, (iii) complete disappearance (broadening) of the Mn^{2+} spectrum for $\mathbf{H} \| \hat{\mathbf{z}}$, and (iv) a stronger crystal field, compared to that in other Tutton salts. He concluded that the interaction between the host Ni^{2+} ions with the impurity Mn^{2+} ions was responsible for these features. Misra and Mikolajczak[3] extended the X-band EPR measurements on NiASH from room to liquid-helium temperature (LHT) in order to study the variation of linewidth as a function of temperature and the orientation of $\mathbf{H}$, as well as to determine the absolute signs of the SHP's. Although they estimated the parameters by numerical diagonalization of the SH matrix, the method used was not particularly suitable to the electron-nuclear spin-coupled system of Mn^{2+}.[6] Furthermore, the sample used was of arbitrary shape, not enabling the determination of Mn^{2+}-Ni^{2+} exchange interaction in NiASH, since the shape-dependent g shift could not be estimated. The only EPR studies on Mn^{2+}-doped $Co(NH_4)_2(SO_4)_2 \cdot 6H_2O$ (hereafter CoASH) have been reported by Upreti,[4] he made measurements at X band in the temperature range 90—373 K. He found that the linewidth increased as the temperature was decreased, which he attributed to the increased magnetic interaction between the host Co^{2+} and the impurity Mn^{2+} ions as the temperature was decreased. In Ref. 4, the SHP's were estimated by the use of perturbation expressions and the line positions as observed for $\mathbf{H}$ along the three principal axes. As for Mn^{2+}-doped $Cd(NH_4)_2(SO_4)_2 \cdot 6H_2O$ (hereafter CdASH), X-band room-temperature studies have been published by Jain;[5] he estimated the SHP's by the use of second-order perturbation expressions from the line positions obtained for $\mathbf{H}$ along the principal axes z and x; the absolute signs of the parameters could not be determined because he did not make measurements at liquid-helium temperature. Strach and Bramley[7] have recently presented their zero-field EPR (ZFR) measurements on four Tutton salts, not including NiASH, CdASH, or CoASH. They determined accurate values of SHP from their ZFR (zero-field resonance) data; as well, they attempted to resolve the ambiguity in the sign of the parameter b_2^0, which was apparently caused by the different choices of the z axis of the b_2^m tensor in previously reported investigations; see, e.g., Bleaney and Ingram[8] for the cases of Mn^{2+}-doped $Zn(NH_4)_2(SO_4)_2 \cdot 6H_2O$ (ZnASH) and $Mg(NH_4)_2(SO_4)_2 \cdot 6H_2O$ (MgASH). Strach and Bramley[7] also noted that the values of the Mn^{2+} SHP's b_4^0 and b_4^2 for NiASH, as reported in Ref. 3, were one to two orders of magnitude larger than those estimated by them for ZnASH and MgASH from ZFR data.

The purpose of the present paper is to report further detailed X-band EPR studies on Mn^{2+}-doped NiASH, CoASH, and CdASH single crystals at room, liquid-nitrogen (LNT), and liquid-helium temperatures. The main objectives are (i) to determine the absolute signs of SHP's from liquid-helium temperature spectra; (ii) to estimate the average nearest- and next-nearest-neighbor Mn^{2+}-Ni^{2+} exchange interaction in the NiASH host, using the g shift at liquid-helium temperature from that in isostructural diamagnetic hosts [in order to accomplish this, it was necessary to use a crystal with a well-defined shape, for Kittel[9] has shown that the particular shape of the host crystal containing paramagnetic ions also causes a g shift due to the magnetization of the host crystal, over

and above that due to exchange interaction with the host paramagnetic ions, equal to $(4\pi/3-N_z)3M/2H$, where N_z is the demagnetization factor along the axis of symmetry (equal to $4\pi/3$ for a spherical sample) and M is the magnetization—thus, in order to determine this, a spherical NiASH sample was used in the present investigations, for which the shape-dependent g shift is zero]; (iii) to study the linewidth variation as a function of temperature, as well as a function of the magnitude and orientation of **H**; and (iv) to estimate more accurately the SHP's by the use of a rigorous least-squares fitting procedure, employing simultaneously the resonant line positions observed for many orientations of the external magnetic field. (To this end, a recently developed computer technique,[6] diagonalizing the SH matrix numerically, especially adapted to the electron-nuclear spin-coupled system of Mn^{2+}, was utilized.)

This paper is a sequel to a recently published study on Mn^{2+}-doped ZnASH, MgASH, and $Fe(NH_4)_2(SO_4)_2\cdot 6H_2O$ (FeASH).[10] Mn^{2+}-Ni^{2+} exchange interaction has been previously estimated from the g shifts in paramagnetic hosts from those in isostructural diamagnetic hosts at liquid-helium temperatures.[11–13] g shifts have also been used to estimate the Gd^{3+}-Yb^{3+} exchange interaction in $LiYbF_4$.[14]

II. g SHIFT, SAMPLE PREPARATION, CRYSTAL STRUCTURE, SPIN HAMILTONIAN, AND EXPERIMENTAL ARRANGEMENT

For the paramagnetic host NiASH, a spherical sample of appropriate size (about 3 mm diameter) was used. (Thus, as discussed in the Introduction, the shape-dependent g shift is zero for this sample.) However, there is another g shift experienced by Mn^{2+} ions in this host; it is caused by the exchange interaction with the paramagnetic host ions Ni^{2+}, which can be expressed as (see the Appendix and Ref. 15)

$$\Delta g = g_p - g_d = -Jn'/\mu_B H \ . \tag{2.1}$$

In Eq. (2.1), g_p, g_d, J, and n' represent, respectively, the Mn^{2+} g factor in NiASH, Mn^{2+} g factor in a diamagnetic host isostructural to NiASH, Mn^{2+}-Ni^{2+} nearest-neighbor exchange interaction in NiASH, and the number of nearest and next-nearest Ni^{2+} neighbors to Mn^{2+}.

The samples were prepared by slow evaporation of aqueous solutions of appropriate Tutton salts containing a sufficient amount of $MnSO_4\cdot H_2O$ so as to provide one Mn^{2+} ion for every 1000 Ni^{2+}, Co^{2+}, or Cd^{2+} ions in the respective solutions. The spherical NiASH sample was prepared by blowing a sufficiently large crystal on emery paper.

The crystal structure of the Tutton salts is monoclinic, characterized by the space group $P2_1/a$, with two molecules per unit cell. The unit-cell parameters are roughly in the ratio 3:4:2, while the angle β is close to 105°. In particular, for NiASH,[16] $a=9.24$, $b=12.54$, $c=6.24$ Å, $\beta=106°58'$; for CoASH,[17] $a=9.25$, $b=12.52$, $c=6.24$ Å, $\beta=107°6'$; and for CdASH,[18] $a=9.43$, $b=12.82$, $c=6.29$ Å, $\beta=106°52'$. The divalent metal ions in the Tutton salts are located at the positions (0,0,0) and $(\frac{1}{2},\frac{1}{2},0)$ in the unit cell and are surrounded by octahedra of six water molecules.

The spin-Hamiltonian appropriate to the Mn^{2+} EPR spectrum in the Tutton salts is expressed in the usual notation as follows:[5,8,9]

$$\begin{aligned}\mathcal{H} = {} & \mu_B \mathbf{S}\cdot\tilde{g}\cdot\mathbf{H} + \sum_{m=0,2} \tfrac{1}{3} b_2^m O_2^m + \sum_{m=0,2,4} \tfrac{1}{60} b_4^m O_4^m \\ & + AS_zI_z + B(S_xI_x + S_yI_y) + Q'[I_z^2 - \tfrac{1}{3}I(I+1)] \\ & + Q''(I_x^2 - I_y^2) \ . \end{aligned} \tag{2.2}$$

In Eq. (2.2), $\tilde{g}$, μ_B, S $(=\frac{5}{2})$, I $(=\frac{5}{2})$, and O_l^m are, respectively, the electronic g matrix, the Bohr magneton, electron spin, nuclear spin, and the electron spin operators (as defined by Abragam and Bleaney[19]). Q' and Q'' cannot be determined from the "allowed" line positions ($\Delta M=\pm 1$, $\Delta m=0$; M and m are the electronic and nuclear quantum numbers, respectively), as the corresponding resonant line positions do not depend upon them. The x,y,z axes corresponding to a Mn^{2+} ion are defined to be the principal axes of the b_2^m tensor, such that the three extrema in the overall splittings of EPR spectra are obtained for **H** along $\hat{\mathbf{z}}$, $\hat{\mathbf{x}}$, and $\hat{\mathbf{y}}$ in decreasing order of the overall splittings.

A Varian V4506 X-band spectrometer was used for EPR measurements, while the magnetic field was measured using a Bruker gaussmeter (B-NM20). For more details, see Ref. 9.

III. EPR SPECTRA

The features of the EPR spectra as observed for the three hosts are as follows.

A. NiASH

At room temperature two sets of spectra corresponding to two physically inequivalent, but magnetically equivalent, Mn^{2+} ions were observed. In particular, for the orientation of **H** between 90° and 95° from the z axis

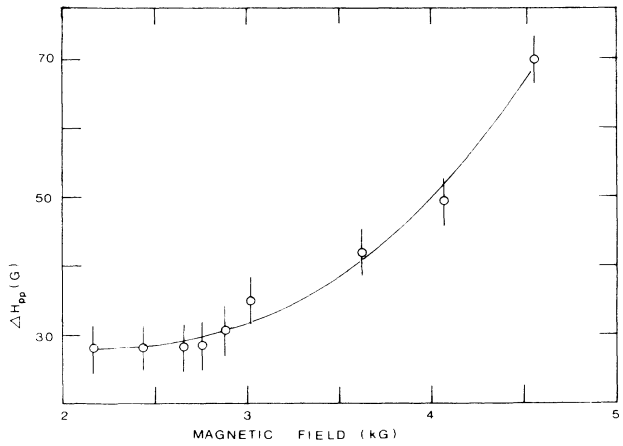

FIG. 1. Peak-to-peak linewidth of the first-derivative line shape as a function of the magnitude of **H** at room temperature for $\mathbf{H}||\hat{\mathbf{x}}$ for Mn^{2+}-doped NiASH.

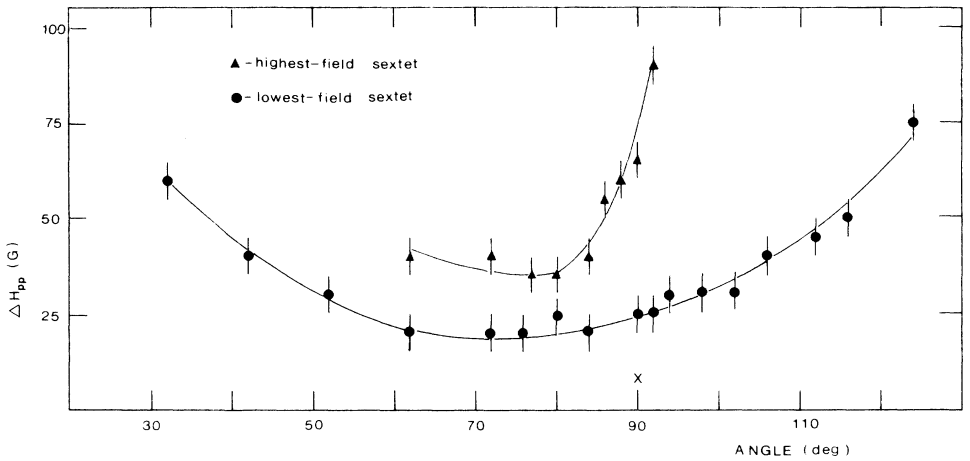

FIG. 2. Average peak-to-peak linewidth of the first-derivative line shape for the lowest- and highest-field sextets as functions of the orientation of **H** in the *zx* plane at room temperature for Mn^{2+}-doped NiASH.

in the *zx* plane, all 30 hyperfine lines for Mn^{2+} ions were observed, the highest-field sextet was observed only for the orientation of **H** from about 90° to 120° and from about 20° to 34° from the *z* axis in the *zx* plane. Likewise, the two lowest-field sextets could be observed only for the orientation of **H** from about 45° to 128° from the *z* axis in the *zx* plane. For more details, and a plot of angular variation of spectra, see Ref. 3. These features remained the same as the temperature was lowered to the liquid-helium temperature, except for (i) additional observation of the two lowest-field sextets for the magnetic field orientation from about 45° to 150° from the *z* axis, and (ii) the disappearance of the highest-field sextet for the magnetic field orientation along the *x* axis at 85 K (this sextet reappears at liquid-helium temperature). As for the linewidths in the NiASH host, the following observations are made: (i) the average linewidth of the EPR lines in NiASH is greater than those in CdASH and CoASH at all temperatures, and (ii) the average linewidth is dependent on both the orientation and the magnitude of **H**. Figure 1 exhibits the linewidth in NiASH as a function of the magnitude of **H** at room temperature for $\mathbf{H}||\hat{\mathbf{x}}$; it is easily seen that there is a monotonic increase of linewidth with increasing magnitude of **H**. The average room-temperature linewidths for the lowest- and highest-field sextets as functions of the orientation of **H** in the *zx* plane are shown in Fig. 2; it is evident that these linewidths are quite anisotropic.

B. CdASH

At all temperatures, the spectra are typical of two physically inequivalent, but magnetically equivalent, Mn^{2+} ions; all 30 hyperfine "allowed" lines could be observed at all orientations of the external magnetic field. The room-temperature angular variation of EPR spectra is similar to that observed for CoASH at room temperature, exhibited in Fig. 3. As has been observed for Mn^{2+}-doped FeASH, ZnASH, and MgASH host crystals,[9] the overall splittings of spectra for $\mathbf{H}||\hat{\mathbf{z}}$ remains almost the same as the temperature is lowered from room temperature to LHT, while that for $\mathbf{H}||\hat{\mathbf{x}}$ increases monotonically with decreasing temperature. Finally, at 210 K, the overall splitting for $\mathbf{H}||\hat{\mathbf{x}}$ becomes equal to that for $\mathbf{H}||\hat{\mathbf{z}}$. Below 210 K, the overall splitting of lines for $\mathbf{H}||\hat{\mathbf{x}}$ surpasses that for $\mathbf{H}||z$. This temperature behavior of overall splittings for $\mathbf{H}||\hat{\mathbf{z}}$ and $\mathbf{H}||\hat{\mathbf{x}}$ is similar to that displayed for the FeASH host in Ref. 9. The Mn^{2+} linewidths in the CdASH host do not appreciably change, either with the magnitude or with the orientation of **H**, or with the temperature, being 12 ± 3 G. This behavior is the same as those for the other isostructural diamagnetic hosts ZnASH and MgASH.[9]

C. CoASH

Figure 3 exhibits the room-temperature angular variation of EPR spectra for the orientation of **H** in the *zx* plane for one of the physically inequivalent Mn^{2+} ions. The general features of the Mn^{2+} EPR spectra in this paramagnetic host are the same as those in the diamagnetic host CdASH described above, except for the increase in the linewidth with the decrease in temperature. The overall splitting of lines for $\mathbf{H}||\hat{\mathbf{x}}$ is found to increase much more substantially than that for $\mathbf{H}||\hat{\mathbf{z}}$. While the overall splitting for $\mathbf{H}||\hat{\mathbf{x}}$ is smaller than that for $\mathbf{H}||\hat{\mathbf{z}}$ at room temperature, it surpasses that for $\mathbf{H}||\hat{\mathbf{z}}$ below 190 K. The EPR linewidth continues to increase as the temperature is lowered, however, all 30 hyperfine lines are certainly clearly observed down to 115 K. Below 85 K the spectrum completely disappears. This is in agreement with the observation of Upreti.[4] The average linewidth of the various sextets is given in Table I at various temperatures. From this table it is clear that, at all temperatures, the linewidth increases on going from the outer fine-structure groups towards the central group. This is in accordance with the observations of Saraswat and Upreti,[20] for both Mn^{2+}-doped CoASH and $CoK_2(SO_4)_2\cdot 6H_2O$ single crystals. This behavior of linewidth is similar to that caused due to lifetime broadening, explained quantitatively by Mehran *et al.* for Gd^{3+}-doped $EuAsO_4$ and $EuVO_4$

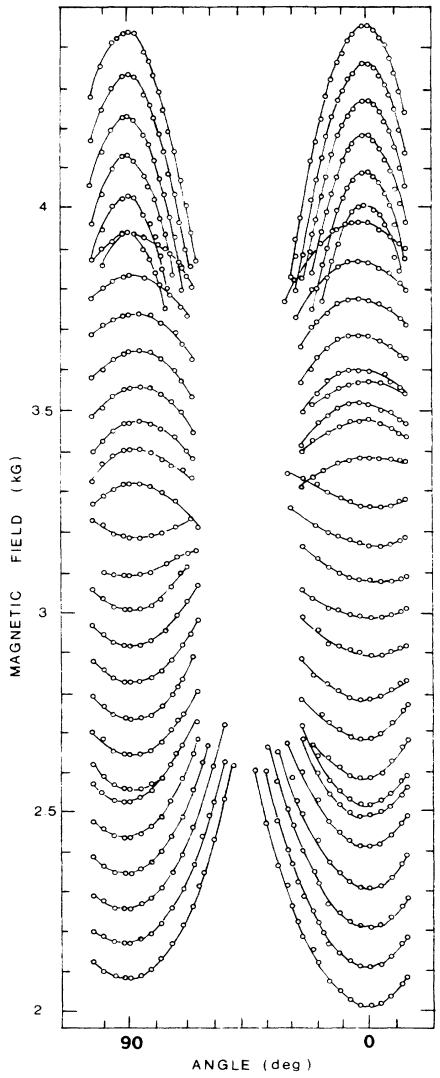

FIG. 3. Angular variation of X-band spectra in the zx plane for one of the physically inequivalent, but magnetically equivalent, sites for the CoASH host at room temperature. The circles represent experimental line positions, while the solid lines are smooth curves that connect data points from the same transition.

single crystals.[21] Indeed, the ratio of the average linewidth of the sextet V to that of the sextet IV, after subtracting off the linewidth in the diamagnetic host CdASH, at 135 K, is 0.6, equal to that predicted by dipolar—exchange-lifetime broadening.

IV. SPIN-HAMILTONIAN PARAMETERS

A. Absolute signs

1. CdASH

The intensity of the highest-field sextet relative to the lowest-field sextet for $\mathbf{H}||\hat{\mathbf{z}}$ for the CdASH host clearly decreases significantly as the temperature is decreased from room to liquid-helium temperature. This indicates a negative absolute sign for the parameter b_2^0 for Mn^{2+} in CdASH.[19] It is also in accordance with the sign as revealed by the spread of the various sextets as a function of $\mathbf{H}$ for $\mathbf{H}||\hat{\mathbf{z}}$. This spread decreases with increasing magnitude of $\mathbf{H}$ indicating that the absolute signs of b_2^0 and A are the same.[6] Since the relative signs of the fine-structure parameters as evaluated from the data are correct, the absolute signs of all the fine-structure parameters can be ascertained with the knowledge of the absolute sign of b_2^0. As for the absolute signs of the hyperfine parameters, they are chosen to be negative for both A and B in accordance with the hyperfine-interaction data.[22] Finally, the eigenvalues as functions of magnitude of $\mathbf{H}$ were numerically computed with this choice of signs of parameters at LHT. Indeed, from these eigenvalues it was found that the highest-field transitions occur among the highest-lying energy levels, confirming the experimental observation that at LHT the intensities of the highest-field lines decrease relative to those for the lowest-field lines for $\mathbf{H}||\hat{\mathbf{z}}$. For, the Boltzmann-population factors are rather small for highest levels as compared with those for the lowest-lying levels at LHT.

2. CoASH

Because of the unavailability of LHT spectra for CoASH, the absolute sign of b_2^0 for this host could not be determined. It has been assumed to be negative, the same as that for CaASH, as indicated by the spread of the various sextets for $\mathbf{H}||\hat{\mathbf{z}}$ and negative absolute signs for the

TABLE I. The average linewidth (in G) of the various sextets $\mathbf{H}||\hat{\mathbf{z}}$ at various temperatures. The linewidth for the central fine-structure group III could not be measured accurately because of overlap of the spectrum due to the other physically inequivalent ion. The various fine-structure groups are labeled in increasing value of H as I, II, III, IV, and V. Dashes denote that these values cannot be determined from the data.

Temperature (K)	I	II	III	IV	V
295	15±3	19±3	—	19±3	15±3
185	18±3	24±3	—	24±3	18±3
155	24±3	36±3	—	36±3	24±3
135	30±3	42±3	—	42±3	30±3
115	42±3	51±3	—	49±3	42±3

hyperfine parameters A,B, determined from the hyperfine-interaction data.[22]

3. NiASH

The lines corresponding to the highest-field sextet for $\mathbf{H}||\hat{\mathbf{x}}$ in this host are rather weak at room and at liquid-helium temperatures. (At liquid-nitrogen temperature they even disappear.) It was, therefore, quite difficult to use the relative-intensity data to unequivocally determine the absolute sign of the parameter b_2^0. On the other hand, the spread of the various sextets as functions of the magnitude of $\mathbf{H}$ increases as the magnitude of $\mathbf{H}$ increases, indicating that the absolute sign of the transformed parameter $b_2^0(x)$ as $z \rightarrow x$ is opposite to that for the hyperfine parameter B. Since the signs of the parameters A,B are negative, as found from the hyperfine-interaction data.[20] This also indicates that the absolute sign of $b_2^0(z)$ in NiASH is negative.

B. Values of the parameters

The technique of the analysis to evaluate SHP's has been well described in Ref. 6, while its application to EPR of Mn^{2+} in the Tutton salts ZnASH, FeASH, and MgASH has been illustrated in Ref. 10. Table II lists the values of the SHP's for the Tutton salts CdASH and CoASH, while the respective values for the NiASH host are listed in Table III at various temperatures. From Table III, it is seen that the g values in the paramagnetic host NiASH are smaller than those in the isostructural diamagnetic host CdASH. This is a feature common to the paramagnetic hosts containing Ni^{2+} ions; e.g., in Mn^{2+}-doped $NiK_2(SO_4)_2 \cdot 6H_2O$,[11,23] $NiSO_4 \cdot 7H_2O$,[12] and $Ni(CH_3COO)_2 \cdot 4H_2O$.[13] It is also noted from Tables II and III that there is a much greater change in the magnitude of the ratio (b_2^0/b_2^2) in the NiASH host as compared with that in the CdASH host as the temperature is lowered from room to liquid-helium temperature.

V. ESTIMATION OF Mn^{2+}-Ni^{2+} EXCHANGE INTERACTION

There are two nearest neighbors (NN) and four next-nearest neighbors (NNN). However, the distance of NNN is only about 20% greater than that for NN. Thus, on the average, n', to be used in Eq. (2.1), expressing the g shift in the paramagnetic host, has been chosen to be 6. It is to be further noted that the error in the value of g_{zz} (Table III) is about 20 times that for g_{xx} because of the nonobservability of the spectrum for the orientation of $\mathbf{H}$ close to $\hat{\mathbf{z}}$. For this reason, the shift in g_{xx} has been used to estimate Mn^{2+}-Ni^{2+} exchange interaction in NiASH. As for the value of g_{xx} in the isostructural diamagnetic host is concerned, the average of the g_{xx} values in the hosts ZnASH,[10] MgASH,[10] and CdASH (2.004, 2.005, and 2.000, respectively) has been used. Using Eq. (A3) of the Appendix the value of the exchange interaction averaged over NN and NNN is estimated to be 0.009 GHz.

The exchange interaction J depends on interatomic distance R as R^{-12} as found by Shrivastava and Jaccarino.[25] It was later found by Shrivastava[26] that an exponential function $J = J_0 e^{-bR}$, with $b = 3.55$, works better than the power law for a number of systems. The exchange was also calculated as a function of bond angles.[26] The paramagnetic shift[27] in the g values may be used to estimate the Mn^{2+}-Ni^{2+} exchange interaction in NiASH. In the present paper, it is estimated that the shift arises mostly from the nearest neighbors, as the factor e^{-bR} gives rise to a considerable reduction at distances increased by 20%. Furthermore, the crystal-field splitting for Ni^{2+} in NiASH, $\beta_2^0 = -59.7$ GHz,[28] is much larger than the estimated value of J so that the shifts are so small that they give rise to only approximate estimates of the exchange interaction. It will be of interest to study the pair spectra.[29] It is important to examine the exchange path in $Ni(NH_4)_2(SO_4)_2 \cdot 6H_2O$. The exchange is an indirect exchange interaction through one,

TABLE II. Values of the spin-Hamiltonian parameters for Mn^{2+}-doped CdASH and CoASH hosts (0.1% doping for each). The parameters b_l^m, A, and B are expressed in units of GHz. The indicated errors are as estimated by use of a statistical method (Ref. 24). The parameters reported by other workers have also been included for comparison. n is the number or lines simultaneously fitted for the evaluation of parameters. Dashes indicate that these values have not been determined.

	CdASH				CoASH	
	5 K[a]	85 K[a]	295 K[a]	298 K[b]	295 K[a]	RT[c]
g_{zz}	2.000±0.001	2.009±0.001	2.003±0.001	2.0168±0.001	2.002±0.001	2.005±0.001
g_{xx}	2.000±0.001	2.003±0.001	2.001±0.001	2.0204±0.002	2.004±0.001	$g_x = 2.009 \pm 0.001$
						$g_y = 2.012 \pm 0.001$
b_2^0	−0.715±0.001	−0.697±0.001	−0.709±0.001	−0.750±0.006	−0.712±0.001	−0.693±0.003
b_2^2	0.863±0.002	0.875±0.002	0.642±0.002	0.150±0.015	0.630±0.002	0.589±0.003
b_4^0	0.002±0.001	0.002±0.001	0.008±0.001	—	0.010±0.001	
b_4^2	0.010±0.013	0.009±0.009	0.026±0.011	—	0.038±0.013	
b_4^4	0.035±0.013	0.073±0.011	0.002±0.011	0.057±0.003	0.006±0.013	
A	−0.273±0.002	−0.276±0.002	−0.276±0.002	−0.267±0.003	−0.270±0.002	$A_z = 0.258 \pm 0.003$
B	−0.262±0.002	−0.251±0.002	−0.251±0.002	−0.264±0.006	−0.270±0.002	$A_x = 0.269 \pm 0.003$
						$A_y = 0.272 \pm 0.003$
n	207	258	229		258	

[a]Present work.
[b]V. K. Jain, Ref. 5.
[c]G. C. Upreti, Ref. 4.

TABLE III. Values of the spin-Hamiltonian parameters for the Mn^{2+}-doped (0.1%) NiASH host. For details and notation, see the caption of Table II.

	5 K[a]	4.2 K[b]	85 K[a]	77 K[b]	295 K[a]	295 K[b]
g_{zz}	1.931±0.040	2.000±0.001	2.022±0.020	1.997±0.001	2.061±0.020	2.000±0.001
g_{xx}	1.992±0.001	2.000±0.001	2.000±0.001	1.999±0.001	2.002±0.001	1.993±0.001
b_2^0	−0.377±0.023	−0.900±0.001	−0.633±0.051	−0.898±0.003	−0.690±0.018	−0.780±0.003
b_2^2	1.242±0.022	0.300±0.003	0.855±0.049	0.295±0.003	0.651±0.016	0.280±0.003
b_4^0	−0.300±0.029	−0.200±0.001	−0.112±0.058	−0.206±0.001	−0.118±0.033	−0.200±0.001
b_4^2	−1.036±0.118	−0.700±0.001	−0.849±0.278	−0.707±0.001	−0.384±0.119	−0.700±0.001
b_4^4	−0.051±0.031	−0.015±0.001	−0.405±0.101	−0.013±0.001	0.033±0.029	−0.015±0.001
A	−0.279±0.016	−0.270±0.001	−0.298±0.005	−0.267±0.001	−0.295±0.007	−0.270±0.001
B	−0.255±0.001	−0.270±0.001	−0.242±0.002	−0.269±0.001	−0.249±0.002	−0.270±0.001
n	246	81	144	70	193	162

[a]Present work.
[b]S. K. Misra and B. Mikolajczak, Ref. 3.

Mn^{2+}-O^{2-}-Ni^{2+}, or two Mn^{2+}-$O^{2-}$$O^{2-}$-$Ni^{2+}$ atoms of O^{2-} which belong to SO_4^{2-} ions, as shown in Fig. 4, on the basis of the crystal structure data of Grimes *et al.*[30] The ligand-ligand overlap is obviously significant in the exchange interaction in the present system.

VI. DISCUSSION

The salient features of the EPR study presented in this paper are as follows.

A. Absolute sign of B_2^0

The absolute sign of b_2^0 has been deduced to be negative in all three hosts CdASH, CoASH, and NiASH. This is in agreement with the absolute sign of b_2^0 in the hosts FeASH, MgASH, and ZnASH.[7,8,10] (For further discussion, see Ref. 10.) This is also in accordance with the absolute sign of b_2^0 as determined by Miedema *et al.*[31] for $Mn(NH_4)_2 \cdot 6H_2O$ from susceptibility measurements.

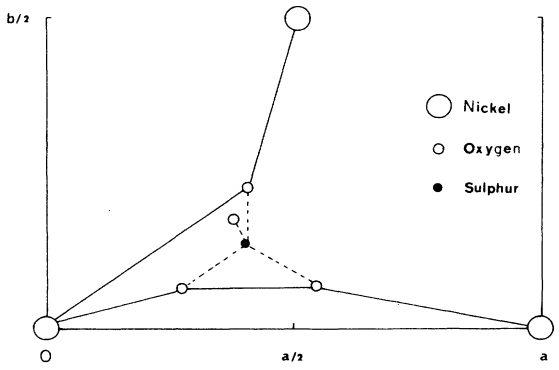

FIG. 4. Projection of the NiASH structure on to the [001] plane, showing three NN and NNN neighbors and one SO_4^{2+} group. The lengths a and b are the unit-cell dimensions. The indirect exchange between Mn^{2+} and Ni^{2+} ions is dominantly via $2s$ and $2p$ orbitals of one or two oxygen ions.

B. Overall splitting of lines for $\mathbf{H}||\hat{\mathbf{z}}$ and $\mathbf{H}||\hat{\mathbf{x}}$

In accordance with the observation for FeASH, MgASH, and ZnASH hosts,[10] it is found that the overall separation of lines for $\mathbf{H}||\hat{\mathbf{z}}$, which is greater than that for $\mathbf{H}||\hat{\mathbf{x}}$ at room temperature, does not change significantly with temperature for CdASH and CoASH. However, the overall separation of lines for $\mathbf{H}||\hat{\mathbf{x}}$ increases substantially with the decrease in temperature, finally surpassing that for $\mathbf{H}||\hat{\mathbf{z}}$ at a certain temperature, typical of the host (Sec. III).

C. Behavior of the linewidth as functions of the orientation and magnitude of H

While there is observed an increase in the average linewidth as the temperature is lowered from room to liquid-helium temperature for the paramagnetic hosts CoASH and NiASH, the linewidth behavior is *very sensitive* to both to the orientation and magnitude of **H** in NiASH. This may be ascribed to be due to the interaction of the probe Mn^{2+} ions with the host Ni^{2+} ions, which are quite paramagnetic in nature (Sec. III). On the other hand, in CoASH a line-broadening effect similar to lifetime broadening is observed.

D. Mn^{2+}-Ni^{2+} exchange interaction

The magnitude of the Mn^{2+}-Ni^{2+} exchange interaction, averaged over the nearest and next-nearest neighbors, has been estimated to be 0.009 GHz in NiASH, as found from the shift of the g factor in NiASH from that in the isostructural hosts CdASH, MgASH, and ZnASH (Sec. V).

ACKNOWLEDGMENTS

The authors are grateful to the Natural Sciences and Engineering Research Council of Canada for financial support (Grant No. A4485). The facilities of the Concordia University Computer Center were used for numerical evaluation of the results presented in this paper. Helpful discussions with Professor K. N. Shrivastava are gratefully acknowledged.

APPENDIX

Assuming a pairwise exchange interaction between a Mn^{2+} ion with its nearest neighbor Ni^{2+}, the total spin Hamiltonian for the pair can be expressed as

$$\mathcal{H}_t=\mathcal{H}+\mathcal{H}'+\mathcal{H}_p ,$$

where

$$\mathcal{H}=g_d\mu_B\mathbf{S}\cdot\mathbf{H}+b_2^0O_2^0+b_2^2O_2^2+b_4^0O_4^0+b_4^2O_4^2+b_4^4O_4^4$$

is the spin Hamiltonian of the Mn^{2+} ion ($S=\frac{5}{2}$) (see Sec. II for further details):

$$\mathcal{H}'=g_1\mu_B\mathbf{S}_1\cdot\mathbf{H}+\beta_2^0O_2^0+\beta_2^2O_2^0$$

is the spin Hamiltonian of the Ni^{2+} ion ($S_1=1$), and $\mathcal{H}_p=J\mathbf{S}\cdot\mathbf{S}_1$ represents the Mn^{2+}-Ni^{2+} exchange interaction, where J is the exchange-interaction constant.

The wave functions of the total system can thus be expressed as product wave functions $\psi_1(M)\psi_2(M')$, where $M=\pm\frac{5}{2},\pm\frac{3}{2},\pm\frac{1}{2}$, and $M'=\pm1,0$. Thus the spin Hamiltonian of the pair system is an 18×18 matrix. If we assume now that the external magnetic field is along the z axis, the following expressions can be obtained, using perturbation theory and neglecting smaller zero-order terms in the spin Hamiltonian of Mn^{2+}, for the lowest-lying Ni^{2+} energy level ($M'=-1$) (Ref. 28) at liquid-helium temperature:

$$E(\tfrac{1}{2},-1)=g_d\mu_BH/2-J/2-g_1\mu_BH-\tfrac{8}{3}b_2^0+\tfrac{1}{3}\beta_2^0+4.5J^2\Big/\left[(g_d-g_1)\mu_BH-\frac{J}{2}+\beta_2^0\right],$$

$$E(-\tfrac{1}{2},-1)=-g_d\mu_BH/2+J/2-g_1\mu_BH-\tfrac{8}{3}b_2^0+\tfrac{1}{3}\beta_2^0+4J^2\Big/\left[(g_d-g_1)\mu_BH+\frac{J}{2}+\beta_2^0-2b_2^0\right].$$

From the above energy levels, using the resonance condition (for the transition $\frac{1}{2},-1\leftrightarrow-\frac{1}{2},-1$) $h\nu=g_p\mu_BH$, one obtains the following expression for the g factor as observed in a paramagnetic host lattice:

$$g_p=g_d-\frac{J}{\mu_BH}+\frac{J^2}{\mu_BH}\alpha , \tag{A1}$$

where

$$\alpha=\frac{[(g_d-g_1)\mu_BH+8.5J-8b_2^0+\beta_2^0]}{2[(g_d-g_1)\mu_BH+\beta_2^0]^2} . \tag{A2}$$

In order to determine J one should solve the quadratic equation (A1). With the approximation $|J|,|(g_d-g_1)\mu_BH|,|b_2^0|\ll|\beta_2^0|$, the only acceptable solution, compatible in magnitude with the molecular-field theory,[32] is

$$J=(g_d-g_p)\mu_BH . \tag{A3}$$

The above solution is also obtained when the term in J^2 in Eq. (A1) is neglected, since $\alpha\ll1$. J in Eq. (A2) should be replaced by Jn' in an average calculation treating the nearest and next-nearest neighbors equivalently, where n' is the number of nearest and next-nearest neighbors.

*Permanent address: Department of Experimental Physics, Maria Curie-Sklodowska University, 20-031 Lublin, Poland.

[1]G. C. Upreti, J. Magn. Reson. **14**, 274 (1974).
[2]G. C. Upreti, Phys. Status Solidi B **56**, K113 (1978).
[3]S. K. Misra and B. Mikolajczak, Phys. Status. Solidi B **96**, 807 (1979).
[4]G. C. Upreti, Chem. Phys. Lett. **18**, 120 (1973).
[5]V. K. Jain, Z. Naturforsch. **32a**, 1364 (1977).
[6]S. K. Misra, Physica **121B**, 193 (1983).
[7]S. J. Strach and R. Bramley, J. Magn. Reson. **56**, 10 (1984).
[8]B. Bleaney and D. J. E. Ingram, Proc. R. Soc. London, Ser. A **205**, 336 (1951).
[9]C. Kittel, Phys. Rev. **73**, 155 (1948).
[10]S. K. Misra and S. Z. Korczak, Phys. Rev. B **34**, 3086 (1986).
[11]S. K. Misra and M. Kahrizi, Phys. Rev. B **28**, 5300 (1983).
[12]S. K. Misra and M. Kahrizi, Phys. Rev. B **30**, 5920 (1984).
[13]S. K. Misra and M. Kahrizi, Phys. Rev. B **30**, 5352 (1984).
[14]S. K. Misra, M. Kahrizi, P. Mikolajczak, and L. Misiak, Phys. Rev. B **32**, 4738 (1985).
[15]Note that the previous estimates of J (Refs. 11–13) were made on the basis of the $M'=0$ level lying lowest for Ni^{2+}; while it is the $M'=-1$ level that lies lowest [see J. H. E. Griffiths and J. Owen, Proc. R. Soc. London, Ser. A **213**, 459 (1952) and K. Ono, J. Phys. Soc. Jpn. **8**, 808 (1953); J. T. Schriempf and S. A. Friedberg, J. Chem. Phys. **40**, 296 (1964).] It should be further noted that there was an error in Eq. (2.3) of Ref. 11; $(g+g_1)$ there should be replaced by $(g-g_1)$. Finally, using Eq. (A3) of the Appendix of the present paper the values for the Mn^{2+}-Ni^{2+} exchange interaction, averaged over NN and NNN, are estimated to be 0.029, 0.037, and 0.009 GHz for $NiK_2(SO_4)_2\cdot6H_2O$, $NiSO_4\cdot7H_2O$, and $Ni(CH_3COO)_2\cdot4H_2O$, respectively. It should be noted that the error in g_{zz} in $NiK_2(SO_4)_2\cdot6H_2O$ was rather large due to the nonobservability of the spectrum for $\mathbf{H}||\hat{\mathbf{z}}$. (About 20 times that for g_{xx}.) Thus the shift in the g_{xx} value in this host has been used to estimate the Mn^{2+}-Ni^{2+} exchange interaction, just as for NiASH in the present paper. In the same way as calculated for Ni^{2+} in the Appendix, if a perturbation calculation is made for Fe^{2+} ($S_1=2$) assuming that its $M'=-2$ state lies lowest [J. C. Gill and P. A. Ivey, J. Phys. C **7**, 1536 (1974)], one obtains $J=(g_d-g_p)\mu_BH/2$. Using this result, and averaging over NN and NNN neighbors, the average Mn^{2+}-Fe^{2+} exchange interaction in $Fe(NH_4)_2(SO_4)_2\cdot6H_2O$ is estimated to be -0.006 GHz, where the g values for $\mathbf{H}||\hat{\mathbf{x}}$ as reported in Ref. 9 have been used.
[16]H. Montgomery and E. C. Lingafelter, Acta Crystallogr. **17**, 1478 (1964).
[17]H. Montgomery, R. V. Chastain, J. J. Natt, A. M. Witkowska, and E. C. Lingafelter, Acta Crystallogr. **22**, 775 (1967).
[18]H. Montgomery and E. C. Lingafelter, Acta Crystallogr. **20**, 728 (1966).
[19]A. Abragam and B. Bleaney, *Electron Paramagnetic Resonance of Transition Ions* (Clarendon, Oxford, 1970).
[20]R. S. Saraswat and G. C. Upreti, Chem. Phys. **23**, 97 (1977).
[21]F. Mehran, K. W. H. Stevens, and T. S. Plaskett, Phys. Rev. B **20**, 1817 (1979).
[22]A. Steudel, *Hyperfine Interactions* (Academic, New York, 1976), p. 182.
[23]S. K. Misra and M. Jalochowski, Physica B **112**, 83 (1982).
[24]S. K. Misra and S. Subramanian, J. Phys. C **15**, 7199 (1982).

[25]K. N. Shrivastava and V. Jaccarino, Phys. Rev. B **13**, 299 (1976).
[26]K. N. Shrivastava, Phys. Status Solidi A **125**, 11 (1984); **125**, 441 (1984).
[27]M. T. Hutchings, C. G. Windsor, and W. P. Wolf, Phys. Rev. **148**, 444 (1966); R. G. Birgneau, M. T. Hutchings, and W. P. Wolf, *ibid.* **179**, 275 (1969).
[28]J. H. E. Griffiths and J. Owen, Proc. R. Soc. London, Ser. A **213**, 459 (1952).
[29]E. A. Harris and J. Owen, in *Electron Paramagnetic Resonance,* edited S. Geschwind (Plenum, New York, 1972).
[30]N. W. Grimes, H. F. Kay, and M. W. Webb, Acta. Crystallogr. **16**, 823 (1963).
[31]A. R. Miedema, J. Van den Brock, H. Postma and W. J. Huiskamp, Physica **25**, 1177 (1959).
[32]S. K. Misra and M. Kahrizi (unpublished).